“A Spatial Approach to Determine Solar PV Potential for Durham Homeowners”

by

Adam Mulherin

May 2011

Approved:

_____

Dr. Lincoln Pratson, Adviser

_____

Date

Master's Project submitted in partial fulfillment of the requirements for the Master of Environmental Management degree in the Nicholas School of the Environment, Duke University

May 2011

Abstract

At present time, solar powered technologies such as photovoltaic (PV) and thermal heating systems supply less than one percent of energy needs in the United States. While conventional forms of energy have proven to be more cost competitive, solar systems can offer a promising alternative. This project examined this viability for a residential neighborhood in Durham, North Carolina. In particular, the analysis focused on the distribution of solar irradiance for fifty homes; each home's distribution was subsequently used to calculate the energy outputs and financial analysis for proposed PV systems as well as determining the best place for each system to be built that will maximize the system's outputs and benefits. This type of analysis was possible by modeling solar radiation in a three dimensional environment that combine remotely sensed data, LIDAR-derived, with the spatial analytical capabilities of GIS. The results from this project will ideally be used as the foundation for an informative tool that will guide homeowners as they make decisions regarding solar PV systems.

TABLE OF CONTENTS

TABLE OF FIGURES

ACKNOWLEGEMENTS

I would like to extend my thanks and gratitude to Dr. Lincoln Pratson who advised me through this Master's Project with guidance and support. Also, I would like to thank a former Nicholas PhD student, Patrick Mahoney, who supplied the LIDAR data necessary to develop my model.

1. INTRODUCTION

Solar radiation is the primary energy source for Earth's physical and biological systems. In fact, it provides over 99% of the energy used to power all natural processes (Pons et al. 2008). Understanding how solar radiation is distributed at specific geographic locations, i.e. mapped, can provide powerful insights into many fields of science, including forestry, ecology, agriculture, etc. Marcel Šúri et al. contend its utility also extends to understanding the potential for renewable energy potential (2007).

One strategy used to study solar radiation in spatial terms has been employed by T. Ramachandra. Over several studies, Ramachandra argues geographic information systems (GIS) offers researchers and managers the tool to understand renewable energy on a spatial scale. GIS' ability to incorporate and synthesize diverse data layers across space is what makes it so valuable (2007). Xavier Pons of the University of Barcelona reaffirms this position. According to his 2008 study, Pons argues "GIS has provided an interesting solution since it allows one to combine digital elevation models (DEMs), numerical modeling, and cartographic tools in the same environment". These abilities give GIS the power to study solar radiation at specific locations.

The methodology presented here uses GIS to map potential solar energy for a residential neighborhood in Durham, North Carolina. Ultimately, the goal of this project is to lay the foundation for a tool that can be used by homeowners to inform decisions regarding photovoltaic (PV) panels on their roof; these decisions include, but are not limited to, how much energy they want the system to produce and cost as well as where the best location is on their roof to maximize outputs. While this project provides an innovate solution, several tools are available online that perform similar types of analysis, such as PV Watts by National Renewable Energy

Laboratory (NREL), the solar calculator at www.findsolar.com, and the Solar PV Financial Calculator developed by North Carolina State University. As a whole, these tools apply generalized information about solar radiation from regional trends to specific homes. While the user is able to adjust particular settings, such as desired energy offsets, solar radiation levels are derived merely from one's zip code. According to Pons, this type of interpolation is "unsuitable for modeling" as each area has its distinctive topography and subsequently solar radiation levels (2008). Lalit Kumar of Sydney University's' School of Geography states "extrapolating is seldom feasible as it is highly variable from place to place due to changing slope (surface gradient) and aspect (surface orientation)" (1997). Another component that these tools do not take into account is the shadows cast from topographic and neighboring features, such as trees and buildings. Shading is a particularly important element in solar energy. The Arizona Research Institute for Solar Energy studied the effects of partial shading on PV systems and found that shade that blocks even ten percent of the incoming light can drop the energy output of a PV system by nearly seventy percent (Thakkar et al. 2009).

This project proposes a promising and robust approach to modeling solar radiation by accounting for shadowing effect and topographic variation at particular locations by incorporating a 3-dimensional technology known as LIDAR (Light Detection and Ranging). LIDAR is a tool used to remotely sense the landscape at very high resolutions (approximately one meter). By collecting data for the terrain and any features above it, LIDAR "offers the possibility to analyze the urban fabric in very innovative ways" (Cernerio et al. 2009). One of those ways is constructing an accurate 3-dimensional model of the urban surface, which includes the ground, buildings, and trees. This urban surface model is an integral component of methodology proposed here to calculate solar radiation at the household level.

By combining LIDAR's urban surface model with GIS' modeling capabilities, this project is able to calculate realistic solar radiation values in a dynamic environment where features interact to create pockets of high and low concentration. Understanding where and how strong these pockets can be a valuable part of the analysis for proposed PV projects. In particular, this analysis is able to show the distribution of solar radiation for a single homeowner's rooftop and subsequently where the best location is to place PV panels. This ability is what makes my approach and tool so unique, valuable, and promising to solar energy projects.

2. STUDY AREA

The methodology proposed here has been developed for a residential neighborhood in Durham, North Carolina. This area sits just north of Duke University and east of its medical campus; a map detailing this context can be seen in the map entitled *Study Area* (see Figure 1). Within this study area, there are approximately three hundred homes. Fifty of these homes were chosen to perform the analysis; these fifty homes are displayed in the map entitled *Study Area (Close-Up)* (see Figure 2). This study area was chosen because it offers an environment where homes and trees are distributed unevenly, i.e. some homes receive significant shading from neighboring trees while other homes are void of such effects. Uneven distribution is an important component for this project since I am studying the various interactions between shadowing effects and potential radiation levels. This area was also chosen for analysis because there was LIDAR data available for analysis, which can be a concern since only seven states have complete data-sets.

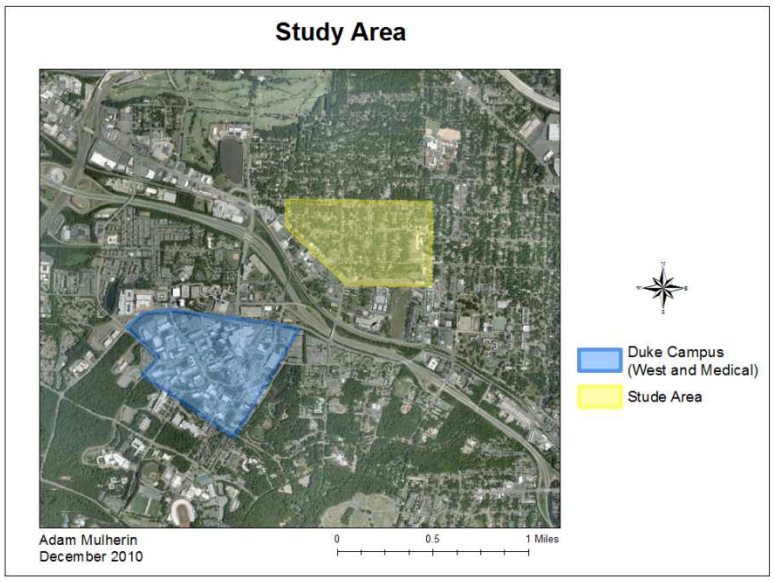

Figure 1 Study Area

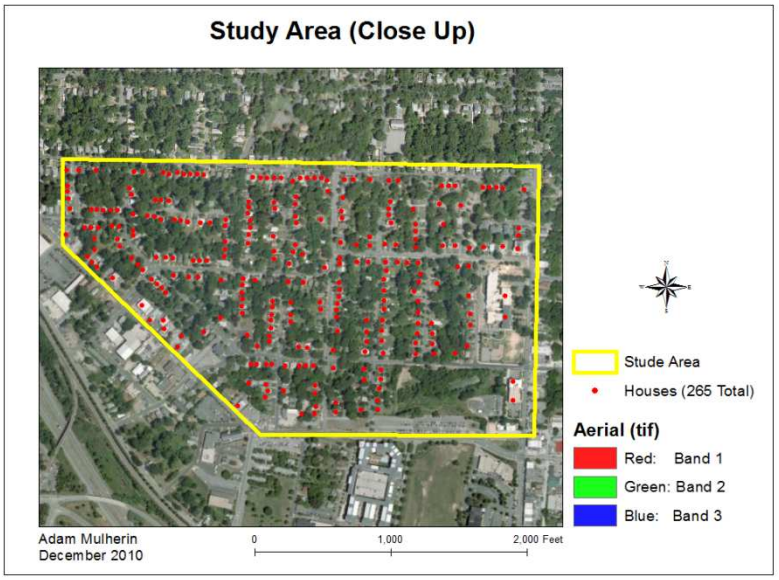

Figure 2 Close-Up of Study Area

1. METHODS

The notion that solar radiation varies spatially has been documented and studied by a number of researchers. According to Thompson, "there is a great variability in the spatial and temporal distribution of solar radiation received at the Earth's surface" (2009). Understanding this distribution is an important component for any methodology that proposes to map potential solar radiation in an urban setting. Consequently, several factors were accounted for in the methodology. In a general sense, these factors can be grouped into two areas: geographic and natural features. The geographic feature of most notable concern is the landscape's topography and associated shadowing effects from the relief's slope and aspects. The interaction between these factors will inherently create areas subject to high or low radiation levels. For example, steeply sloped areas can effect incoming radiation by shading the northern oriented slopes while exposing those that are south-facing. Similar shading effects are experienced when trees block sunlight from reaching the area north of their canopy. This interaction becomes even more significant in an urban setting where trees and homes are often closely spaced.

The methodology proposed here attempts to account for these interactions by constructing an accurate model of the 3-dimensional environment discussed. A remotely sense data set known as LIDAR was used to develop this model. The resulting output was subsequently used as the central component for modeling solar radiation model in GIS. Through various calculations, this and other data were used to create the database and subsequent tool to help inform homeowners' decisions.

1.1 LIDAR Collection

As described earlier, LIDAR is a tool used to remotely sense the landscape. Through a system of airborne sensors and pulsing laser beams, LIDAR is able to "obtain very accurate 3D coordinates (x, y, z) of points located on the surface of the Earth" (Carnerio et at. 2009). In other words, it provides location and elevation data that define the surface of the Earth while providing heights of any features above the ground, such as buildings or trees. These values are obtained by calculating the time elapsed for the beam to return to the plane. Generally speaking, LIDAR comes in two types of data: bare-earth and first-return. Bare-earth refers to the topography, which is typically expressed in digital elevation models (DEMs), whereas first-return data accounts for any features above the bare-earth. The combination of highly accurate DEMs and heights of buildings and trees is what makes LIDAR such a valuable tool for environmental analysis.

The LIDAR data used for my project was obtained through the work done by Patrick Mahoney; Mahoney graduated in 2006 with a PhD from Duke's Nicholas School of the Environment. His work resulted in DEMs at one meter resolution and "first-return" points for particular watersheds in North Carolina. While the DEMs were ready for analysis immediately, the "first-return" data needed to be converted into a usable format. Initially this data was

contained in a raw text file with three columns of information: x-coordinates, y-coordinates, and a z value. The coordinate system used was North Carolina state plan and the z values signify the height of terrain, i.e. topography plus the height of trees and buildings. To convert these three columned data points into a usable format, a python scripting language was used. Essentially this line of code created a shape-file with point features that were assigned a unique x, y, and z value by looping through each line within the raw text file. These points were then uploaded into GIS. By displaying x-y data (a right-click function within GIS), point features were created for each location listed in the text file.

To save time, the LIDAR data was trimmed to the study area discussed earlier and shown in Figure 3. The clipping process can be seen in the model entitled *First Return Clip* (see appendix II). The resulting outputs were a single DEM and first-return points for the study area in questions.

With the point features created and clipped, "first-return" heights were calculated for any obstructions contained within the study area. The map entitled *LIDAR First Return Data Points* details the spatial distribution of a few of these points (see Figure 3). Contained within the study area, there were 297,864 points retrieved from P. Mahoney's data-set that were used for analysis. These points were subsequently interpolated to make a smooth surface.

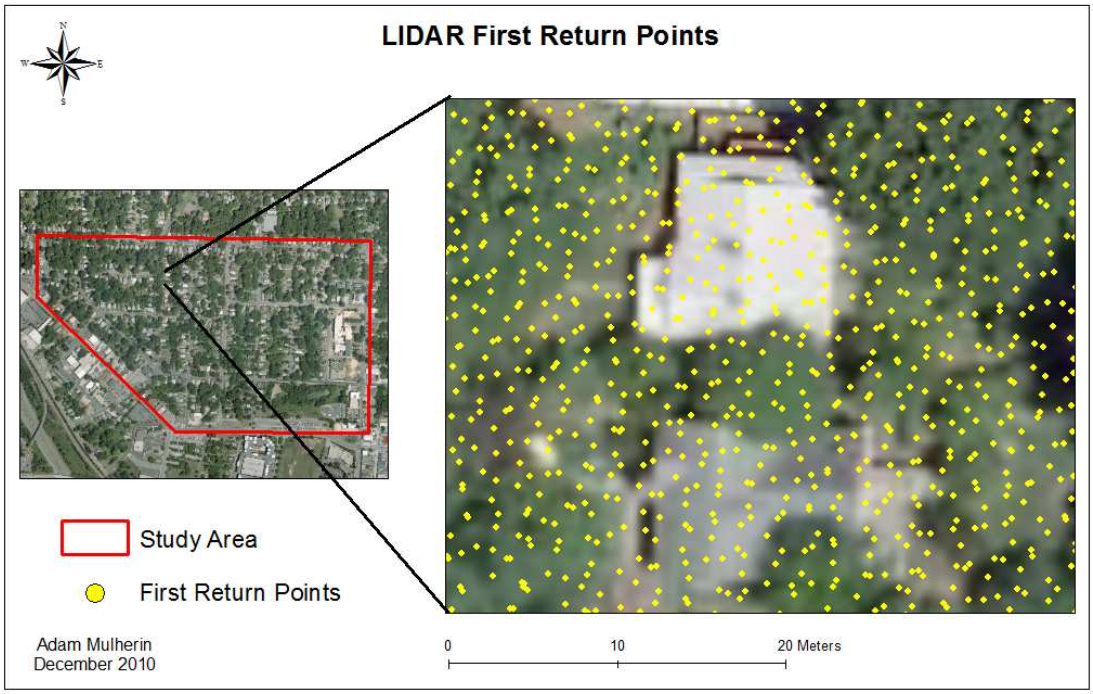

Figure 3 First-Return Data Points for Study Area

Several steps were taken to create a raster surface for the "first-return" data layer. Initially the point features were converted into a Triangulated Irregular Network (TIN). This TIN created a surface with triangles faceted from each respective point feature. To account for the z-values/height of the above-ground features, the TIN was converted into a raster using GIS' Convert TIN to Raster function. This raster created an interpolated surface of the "first-return" data points. The model entitled *Converting First Return to TIN and Raster* depicts this process in greater detail (see appendix II). The map entitled *LIDAR Data for Study Area* (Figure 4) shows the final product of first return data for the study area, as well as the DEM (bare-earth) used. From this map, the urban surface discussed earlier can be seen as building outlines distributed in a grid-like fashion. Furthermore, it should be noted that elevation increased by sixty-five feet from 435 to 500 feet above sea level. This difference can directly be linked to the building and trees above the ground.

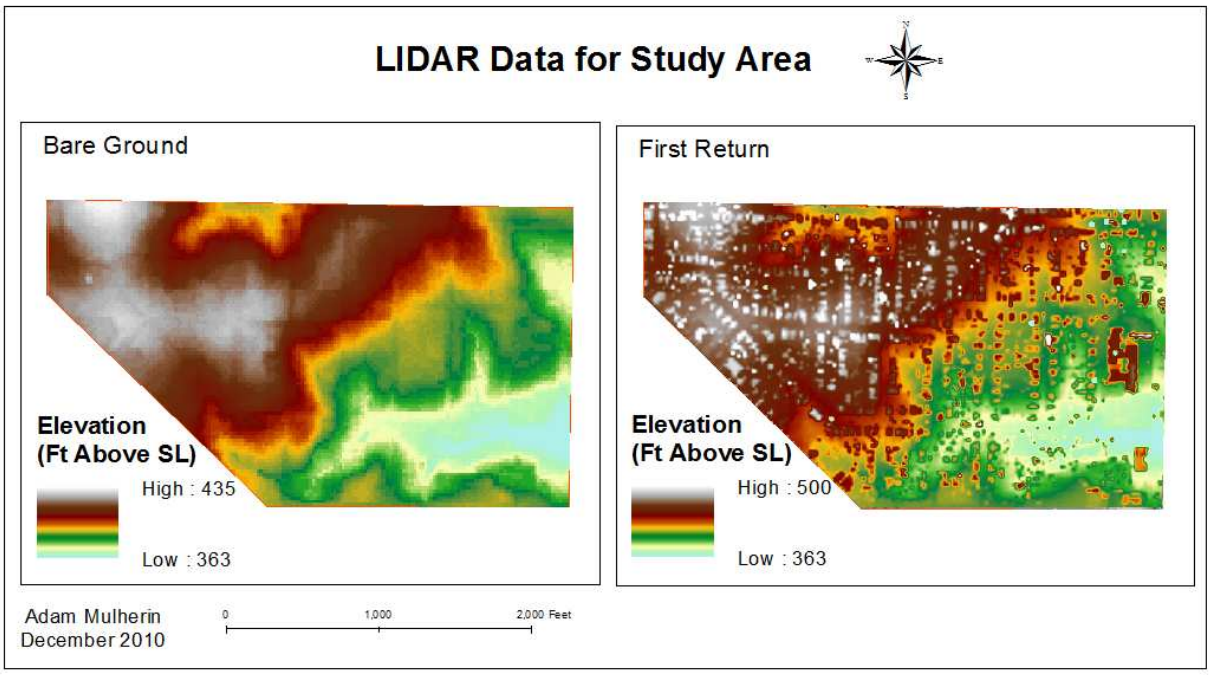

Figure 4 Bare-Earth and First-Return DEMs for Study Area

1.2 Solar Modeling

GIS offers several tools to calculate solar radiation levels, such as point solar radiation and global radiation levels. The global radiation was the tool chosen for the study area. In order to calculate the spatial distribution of solar radiation, both the "bare-earth" and "first-return" layers were used as inputs. Theoretically the level of solar radiation received on rooftops and by association solar panel is the "first-return" raster subtracted from the "bare-earth" raster. In other words, the incoming solar radiation equates to the amount that passes through the air, including open areas and those shaded by trees, until it reaches the ground or rooftop. As such a minus function was used in GIS that subtracted the first-return radiation levels from the bare-earth's. The models entitled *Radiation (Bare-Earth)* and *Radiation (First-Return)* depict these steps in greater detail (see appendix II).

The resulting output was expressed in yearlong averages of incoming solar radiation for each respective pixel. In other words, each pixel represents a unique value. For purposes of comparison, units were converted from Wh/m^2 to W/m^2 by dividing by twenty-four. The map entitled *Average Daily Solar Radiation* depicts these yearlong averages for the study area (see Figure 5).

Since this project's goal was to determine the viability of solar projects for particular houses, the methodology was narrowed to the southern-facing portion of rooftops. Placing panels on the southern side of roofs ensures that the "sunlight strikes the solar collector at a more optimal angle than it would if the collectors are placed on the east, west, or north-facing roof sections" (Bryan et al. 2010). As needed, polygons were made for each rooftop by hand-drawing in each through the use the draw toolbar in GIS; Bing's aerial photograph at 1 meter resolution was used as the points of reference. Solar radiation levels were subsequently extracted for each home in question. This calculation was performed through the use of a statistical tool within GIS called "Zonal Statistics". As detailed in the model entitled *Zonal Statistics*, the variables used were the solar radiation raster for the input value raster and the houses for the feature zone data (see appendix II).

In addition to this information, four more outputs were chosen for analysis: seasonal variations and seasonal extremes. These outputs were deemed important because they are able to tell a homeowner how radiation is expected to differ over time. Over the course of the seasons and within each season, solar radiation can differ drastically as the Earth moves along its rotational orbit. Summer in the Northern Hemisphere coincides with the Northern Hemisphere being oriented more towards the sun, which causes solar rays to strike the ground more directly. Whereas winter in the N. Hemisphere is caused by opposing factors as the Northern Hemisphere

is oriented away from the sun. Within these seasons, there are extremes known as the solstices. The Summer Solstice occurs approximately around June 21st of every year as the North Pole points directly at the sun. On the other side, the Winter Solstice occurs near the 21st of December as the North Pole is pointed directly away from the sun. For these reasons the model was run for summer and winter months as well as for the summer and winter solstices. Within the solar radiation tool, there is a function that manipulates the date/time settings. Whereas previous calculations were defined for all 365 days, the seasonal and solstice calculations manipulated the solar radiation tool by selecting for specific Julian calendar days. For the summer season, days 172 to 265 were selected, which represent June 21st til September 22nd. Similar calculations for the winter season were run as Julian days from 355 to 80 or December 21st to March 21st. These seasonal totals were then converted into seasonal averages by dividing the number of days within each season, 93 and 90 for summer and winter respectively. To account for seasonal extremes, a 24-hour period was selected for both the summer and winter solstice. In this case, Julian days 172 (June 21st) and 355 (December 21st) represented the solstices respectively. These outputs are depicted in the maps entitled *Radiation Levels for Seasons* and *Radiation Levels for Seasonal Extremes* (Figures 7 and 8). As similarly performed above, zonal statistics were used to extract the data for each house. Consequently, these calculations resulted in seasonal averages and extremes for the study area in question.

Calculating seasonal variations was the final step performed in GIS. These values along with the yearlong averages for each respective home were the essential inputs needed to create the informative tool described earlier. Considering this tool aimed to evaluate potential system sizes, electrical outputs, and subsequent cost/benefit analysis, a few other pieces of information were needed, such as local electricity prices, incentives, and technology standards and costs.

Electricity prices for the state of North Carolina were found to be 9.49 cents/kWh according to U.S. Energy Information Administration (EIA), as of January 2010 (http://www.eia.doe.gov/). From the Database of State Incentives for Renewables & Efficiency (DSIRE) local, state, and federal incentives were found. NC GreenPower Initiative offers 19 cents/kWh produced (http://www.dsireusa.org/solar/). This incentive applies to any residential systems under 5kws, which means all fifty homes in question are able to receive this incentive. State incentives for North Carolina residents are thirty-five percent of the total project with an upper limit of $10,500. Similarly, federal incentives reach up to thirty percent of the total project. Together these various incentives translate from a couple thousand to over 20,000 in savings for the respective homeowner, which amounts to nearly 70% of the total cost. Three different technology standards were used to determine each system's output and cost, monocrystalline, polycrystalline, and amorphous thin film. Each technology has its associated efficiency and costs per watt. For purposes of this project, the following standards were used. Monocrystalline solar panels reach efficiencies up to sixteen percent and cost roughly $10.50/watt, whereas polycrystalline panels are twelve percent efficient and cost $9/watt. Lastly, amorphous thin film panels are only 6.5% efficient and cost $7.50/watt. The last piece of input to gather is the local energy mix, which will be used to determine potential pollution abatement. According to the EPA, for each kWh of energy produced in the Durham area, approximately 1.135 pounds of CO^2, 0.00589 pounds of SO^2, and 0.00161 pounds of NO^2 are abated (http://www.epa.gov/cleanenergy/). Together these various inputs were used to calculate the informative tool.

1.3 Tool Creation

To calculate estimated system size and resulting outputs, solar radiation for the entire southern-facing portion of the rooftops were first determined. This calculation was performed by multiplying incoming radiation levels (W/m^2) by the size of each rooftop (m^2). The resulting outputs for each of the fifty homes calculated solar radiation in terms of watts. Watts were then converted to kilowatts by dividing by one thousand. An example of these and all pertinent steps are detailed in Table 2 (see appendix I). Estimated system sizes were subsequently calculated by multiplying the system's total capacity (kW) by the respective efficiencies, which is determined by which technology was chosen. To determine how much electricity can be produced from these systems annually, the respective power values (kW) were converted to energy (W) by multiplying the number of solar peak hours in a day (five) and the number of days in a year (365). Five solar peak hours were deemed appropriate by www.wholesalesolar.com. As a result, the resulting energy outputs were given as kWh/year.

With potential energy outputs determined, total costs for each system were ready to be calculated. As detailed in Table 2, two types of costs were used: before and after incentives (see appendix I). Costs before incentives were calculated by multiplying the expected system size (W) by the respective technologies cost/watt, in this house's case $9/watt were used for polycrystalline panels (http://www.nrel.gov/learning/ 2009). Costs after incentives were calculated by subtracting the local, state, and federal incentives detailed earlier from the total costs before incentives. Cost per watt was also determined by dividing the total power wattage from the total costs.

To accompany these cost outputs, benefits were also determined for each system. These benefits represent how much each system can save a homeowner over a course of a year in terms

of their electric bill. In other words, the electricity produced from their solar panels can offset a certain level of energy normally taken from the grid. Savings for the first year of generation were calculated by multiplying the estimated electricity produced (kWh) by local prices for the Durham area. Subsequent years used a similar methodology while accounting for an annual inflation rate of 3.78%. This inflation rate was consistent with several online sources, such as elitesolar.com and solarcentral.org. Consequently, local electricity prices are expected to increase 3.78% each subsequent year. This procedure was performed for twenty-five years; twenty-five years was chosen because most projects receive a twenty-five year warranty on their solar panels (Green 2005). At the end of the twenty-five year period, total and average savings were calculated by summing the total period's savings and dividing by twenty-five. Expected benefits were then used to determine payback periods for each project. This calculation was performed by dividing total costs by the average annual electrical savings. The resulting outputs represent the number of years it would take for the proposed project to "pay for itself", or when total benefits equal total costs. In addition to the financial costs and benefits, environmental benefits were calculated by multiplying the estimated electricity produced by EPA's pollutant factor, which stands for how much pollution each system can offset by generating electricity off-the-grid.

1.3.1 Example

The progression from these various inputs to the resulting outputs is chronicled for a single home in Table 2 (see appendix I). The first series of calculations were performed to determine how much electricity can be generated from the system; these are detailed in equations one through four. The first step determined total available power for the home by multiplying

the roof's size (m^2) by total radiation (W/m^2), which resulted in total potential power in terms of watts. This value was subsequently converted to kilowatts by dividing by 1,000. From this potential value, the power that the system can realistically produce was determined by multiplying total potential power by the efficiency of the solar panels; in this case, polycrystalline panels was the defined technology with an efficiency of twelve percent. The next calculation converted the system's power to expected generation, i.e. electricity, by accounting for time. Electricity was determined by multiplying power by peak solar hours within a day for this region (five) and the number of days within a year (365). With this last calculation, the amount of electricity (kWh) this homeowner could expect from the system was determined for an entire year.

The next series of calculations listed in equations five through eleven detail the cost-benefit analysis. Costs were calculated for both pre and post-incentives. Pre-incentive cost amounted to the size of the system (in watts) multiplied by the average cost per watt (in $); since polycrystalline panels were used, an average cost/watt of nine dollars was used. From this value, post-incentive cost was calculated by subtracting the appropriate incentives from the pre-incentive cost, i.e. 35% from the state, 30% from the federal govt., and $.19/kWh from NC GreenPower Initiative. As seen in equation seven, cost per watt was calculated by dividing the post-incentive cost by the size of the system. These last two equations detail how much this homeowner can expect to pay for the project in terms of total costs and average. To accompany these values, benefits were calculated over the expected lifetime of the system and on an annual basis. Savings from the first year of generation was calculated by multiplying electricity produced by the electrical price of $.1076/kWh; in other words, this step details how much the homeowner is saving on his/her electrical bill by generating off-the-grid. Savings for each of the

subsequent years (up to twenty-five) were similarly calculated while accounting for the utility's annual inflation rate of 3.78%. Total and average savings were determined by summing the benefits over the life of the system and dividing this sum by twenty-five.

From the costs and benefits discussed, the financial analysis can be performed. As shown in equations twelve through fourteen, several variables were considered for analysis: payback period, Return on Investment (ROI), and Net Present Value (NPV). Payback period was calculated by determining the time required for this system to pay for itself. In other words, how many years it takes for total benefits to equal the financial investment made. This time was calculated by dividing the post-incentive cost by each year's electrical savings until benefits equaled costs. ROI was calculated by dividing the benefits over the life of the system by the initial investment made; the resulting product was presented as a percentage to show this relationship. NPV similarly accounted for benefits and cost by subtracting the purchase price (initial investment) from future cash flows over the twenty-five years. A rate of five percent was used to discount the equation. Together these three variables were used to perform the financial analysis.

For the environmental analysis, the estimated pollution abated from the system generating off-the-grid was calculated for three pollutants: CO^2, SO^2, and NO^2. Abatement was determined by multiplying generated electricity by the savings factor for each pollutant; this factor is provided in units of pounds per kWh with a factor of 1.135 CO^2, 0.00589 for SO^2, and 0.00161 for NO^2. With these last equations, variables were calculated for the environmental, financial, and system analysis for this respective home; these equations were also used for the other forty-nine homes within the study area.

1.4 Data Assumptions

Before proceeding further, the assumptions that this methodology makes need to be detailed. Generally two major assumptions were made involving the first-return LIDAR data and GIS' solar modeling capabilities. The first assumption made was that enough points were collected to create accurate shapes and heights of trees and buildings. This assumption is critical since each point is part of the 3-dimensional landscape where each feature has its own unique size and orientation. If too few points were available for a specific feature, then its output would not render an accurate representation. After considering there were 297,864 points for the study area that has an area approximately 540,000 m^2 (one point for every two squared meters), this concern becomes minimized. The map entitled *LIDAR First Return Data Points* illustrates this concern visually (see Figure 3). The second assumption made was that GIS is capable of modeling radiation over periods of time, i.e. over a day and seasons. According to the research performed by Kumar et al. GIS' solar analyst has this capability by manipulating the solar altitude angle, which is described as the "angular elevation of the Sun above the horizon" (1997). Over a period of a day, this angle increases from zero at sunrise to maximum at midday and subsequently decreases back to zero as it nears sunset. The solar altitude angle adjusts for seasonal variations by declining or inclining slowly over long series of days. In light of this knowledge, the assumptions made appear to be valid and supported.

2. RESULTS

The methodology detailed in section 3 produced results from GIS' solar analyst and subsequently the informative tool. These results and any observations or trends of importance are examined in detail in the following sections.

2.1 Radiation Modeling

From the methodology detailed above, several outputs were created that map the distribution of incoming solar radiation for the proposed study area. For comparison purposes, these outputs are grouped into yearly averages, seasonal averages, and seasonal extremes. See Figures 5 and 6 for yearly averages and Figures 7 and 8 for seasonal averages and extremes on the following pages for detailed maps. Figure 6 illustrates yearlong averages at a larger scale to show the interplay between shading effects and radiation levels.

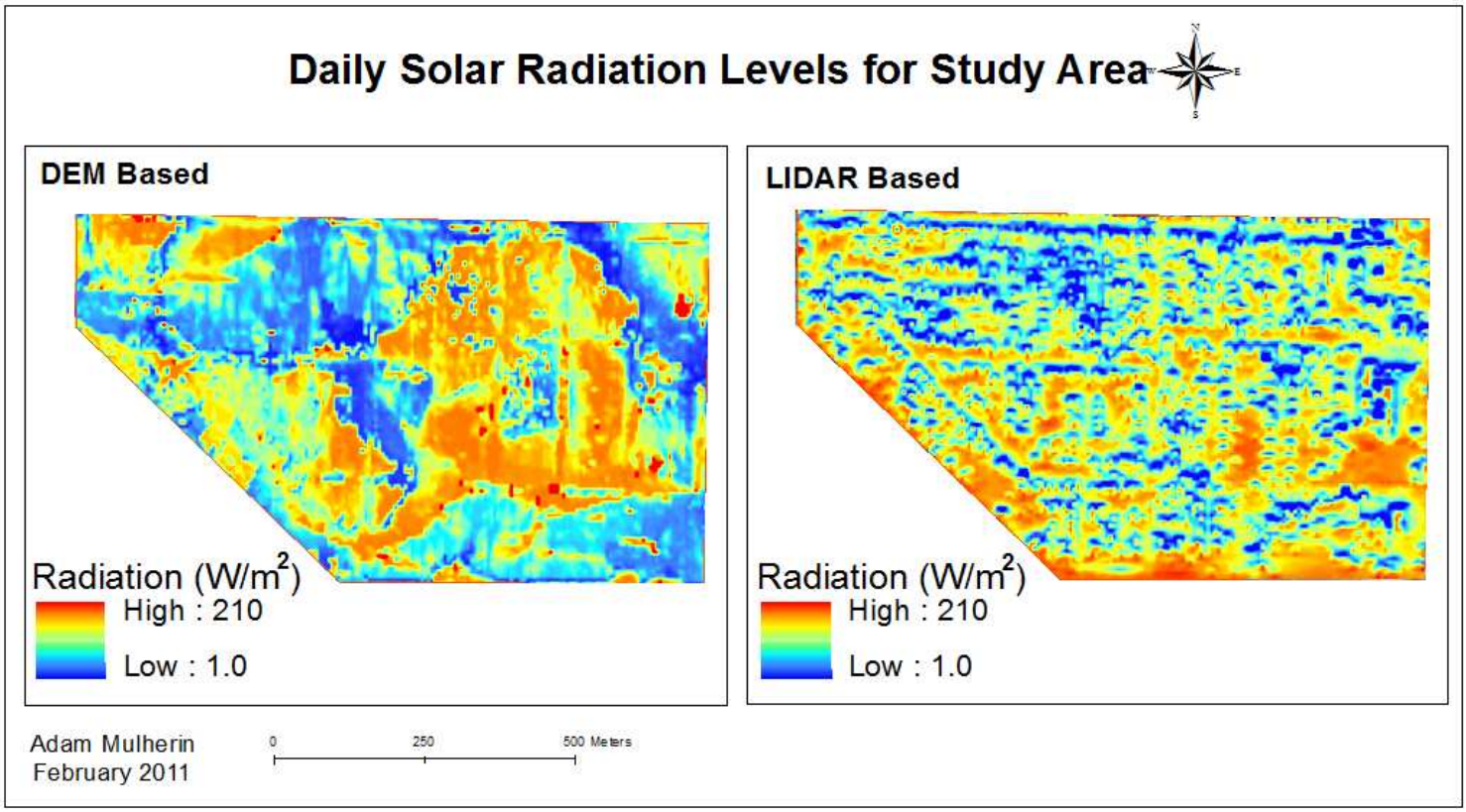

Figure 5 Distribution of Solar Radiation for Study Area

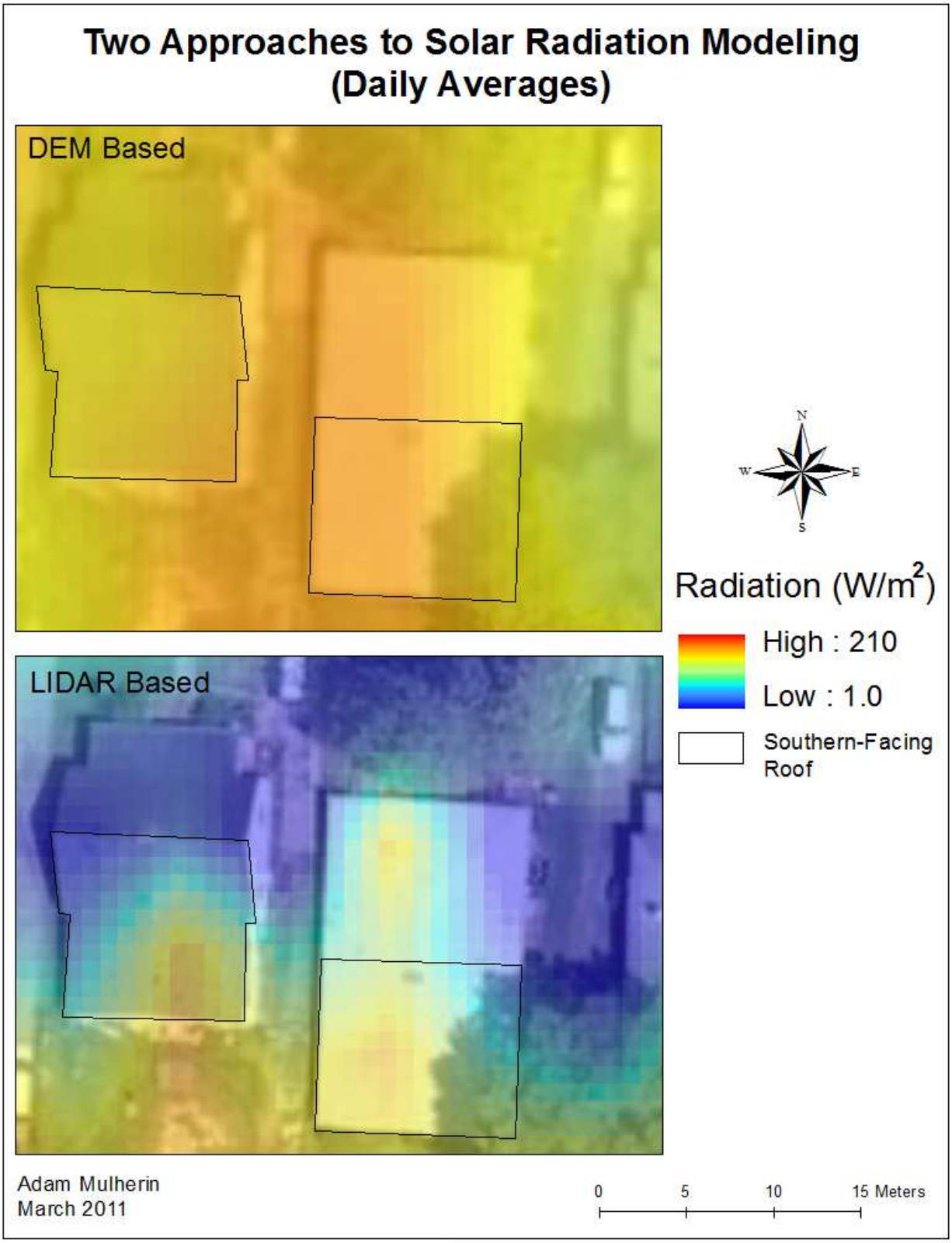

Figure 6 Comparison of Two DEMs in the GIS Model

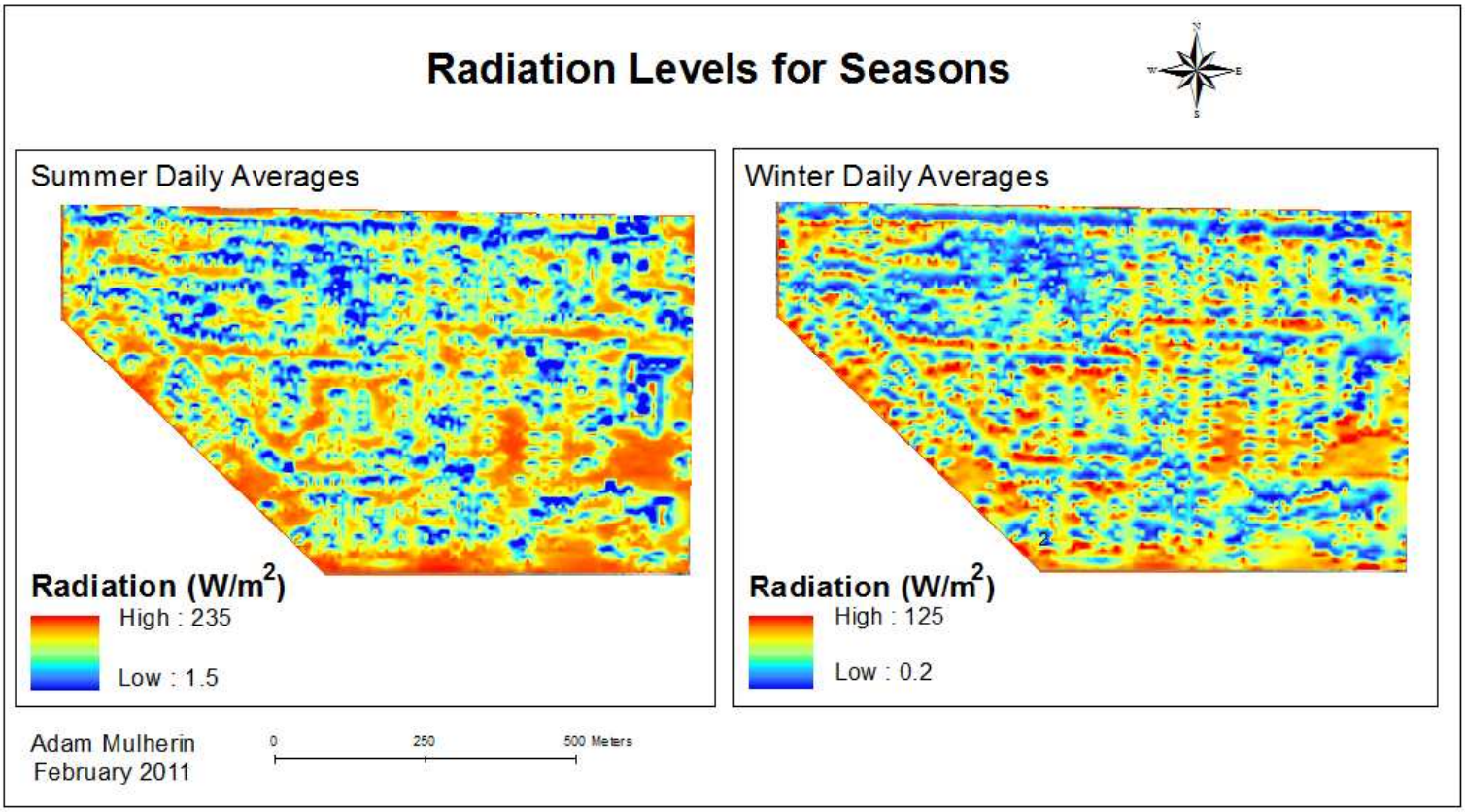

Figure 7 Distributions of Seasonal Averages

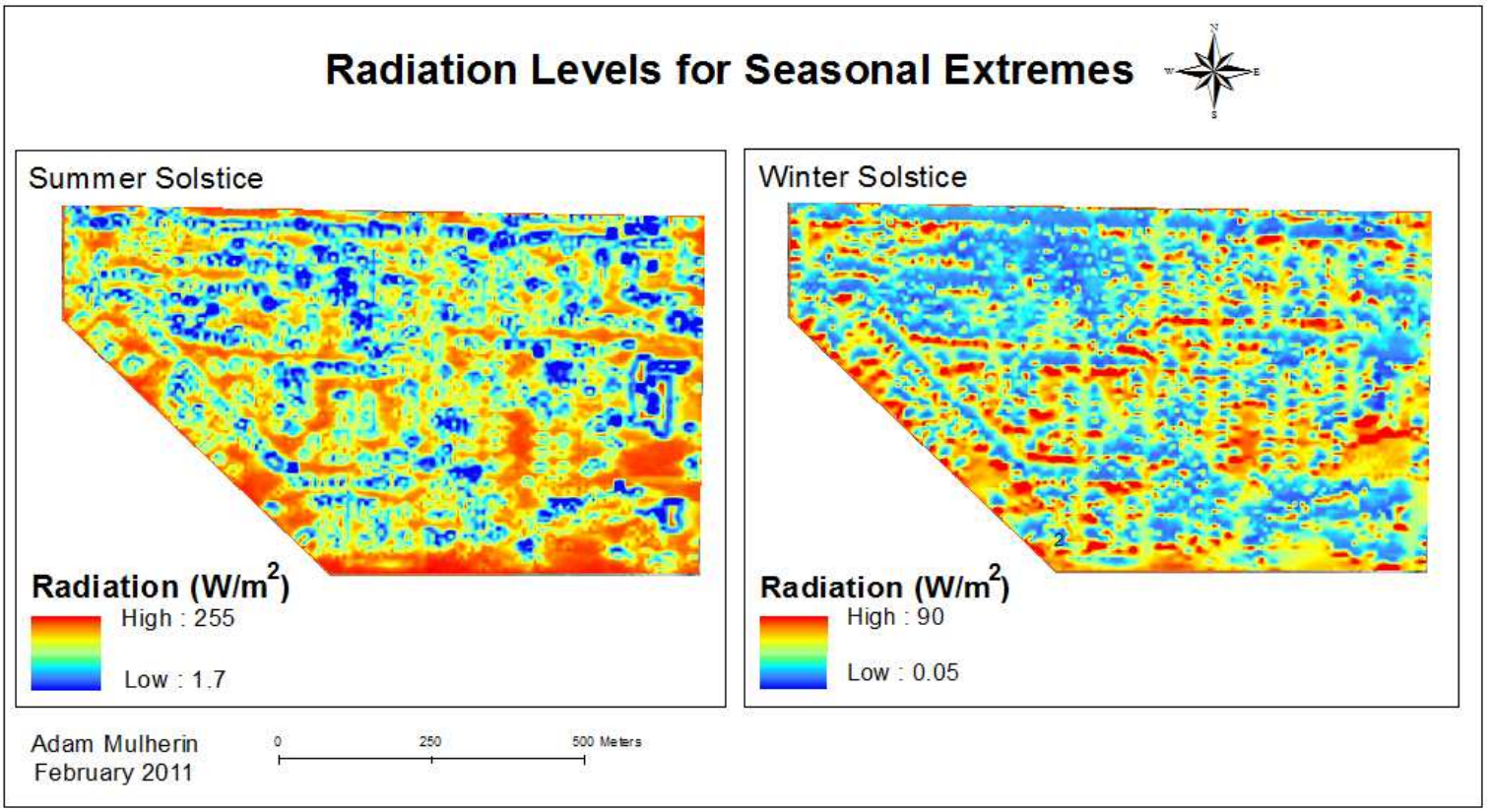

Figure 8 Distributions of Summer and Winter Solstice

The map entitled *Average Daily Solar Radiation Levels for Study Area* represents the distribution of yearlong averages obtained from GIS' solar modeling. The output on the left labeled "DEM Based" was derived by using just the DEM in GIS, while the output labeled "LIDAR Based" was obtained by incorporating the three-dimensional surface from LIDAR's first return data. Consequently, the "LIDAR Based" map accounts for shading effects from obstructing features such as trees and buildings and represents a better distribution of solar radiation. Several important trends and observations are noteworthy when comparing the two maps and examining the later separately. While the radiation gradient remains constant (between 1 and 210 W/m^2), the patterns change significantly. The distribution of the "DEM Based" output shows large areas of either high or low solar concentration. While not completely, these areas appear to generally follow the elevation scale for the study area. More specifically, areas with high levels of solar radiation tend to also be located in places that are more elevated, and vice versa. On the other side, the "LIDAR Based" follows a different pattern. In a general sense, solar radiation is not distributed as evenly as there are many examples of isolated pockets of high or low concentrations. The areas where high and low pockets are spaced closely together appear to follow the housing pattern and grid-like street network characteristic to this neighborhood. Furthermore the larger areas that have consistent levels of radiation coincide with open spaces, such as large yards and parking lots. In both a general and specific perspective, these two outputs render starkly different distributions of solar radiation on a yearlong scale.

These observations are more evident when examining the outputs at a higher scale. The map entitled *Two Approaches to Solar Radiation Modeling* gives a visual depiction of these trends for two homes within the study area. Even within this area that is approximately thirty meters wide, the "DEM Based" distribution is relatively constant while more variation is being

shown in the "LIDAR Based" distribution. Furthermore, the high and low pockets in the "LIDAR Based" output appears to follow closely to the housing structures whereas the "DEM Based" output does not appear to be affected at all by the these features. As was the case at a smaller scale, these outputs differ considerably when examined more closely.

To accompany the yearlong averages, distributions over the summer and winter seasons were also analyzed in the map entitled *Radiation Levels for the Seasons*. As expected, the radiation gradient changes significantly when compared to the yearlong averages. With 1 to 210 W/m^2 being the established range over a year, the range for an average summer day jumps to 1.5 to 235 W/m^2 while an average winter day drops to 0.2 to 125 W/m^2. Both scales differ considerably from the standard set for an entire year. This change is also evident when comparing the "LIDAR Based" patterns to both the summer and winter seasons. While the general trends remain the same during the various time periods, the pockets of high and lows became even more extreme. For example, pockets with high concentration grew in intensity and size during the summer months while low concentrating areas dropped in intensity and grew larger.

Confining time to a smaller window only reaffirms these trends, which is shown in the map entitled *Radiation Levels for Seasonal Extremes*. Similar to previous notions, the highs and lows in these outputs became more extreme as the scales changed to 1.7 to 255 and 0.05 to 90 W/m^2 for the summer and winter solstices, respectively. Moreover, the areas of high concentration became higher and larger during the summer solstice while lower concentrated areas received less radiation and became bigger during the winter solstice. While this logic is intuitive, that areas are going to be warmer when the sun is closer to the Earth and vice versa,

detailing where these trends are located and how strong they are adds a temporal element to the results not typically examined.

In addition to confining time in the GIS model, the impact that shading has on the amount of radiation received can be closely studied by examining these figures closer. The map entitled *Solar Radiation Example* provides the scale to perform this analysis, see Figure 9 below. This image displays daily solar radiation averages over a course of a year imposed onto an aerial photograph to show the houses, streets, and trees. This particular area was chosen as the test site because each house has a unique structure and/or placement relative to the surrounding environment. The two houses on the left appear to not have any trees within roughly twenty meters. However, they differ drastically in structure as the middle house exhibits a greater roof pitch. Whereas the most eastern house appears to have a flat roof with at least one tree able to cast a shadow in the vicinity. Two theories are supported as one examines the visual trends: solar radiation is greatest on the southern-facing portions of roofs and shadows cast from nearby features, i.e. trees or buildings, can limit the level of radiation received. Examining the numbers furthers this support. According to the analysis, the house in the middle which exhibits a steep roof pitch has drastically different radiation values for its north and south-facing portions of the roof; values fluctuate primarily between 100 and 175 W/m^2 for the southern-facing portion while values for the northern-facing portion remained fairly constant around 60 W/m^2 with a few areas nearly reaching 100 W/m^2. While the house on the right appears to have flat roof, which explains the even distribution, a single tree is within shading distance. This effect is shown in the radiation levels as most of the house ranges around 125 to 175 W/m^2 (areas left of the shade) whereas the portion behind the tree drop to as low as 50 W/m^2. Compared to these two examples the house on the left exhibits more of an even distribution as values fluctuate primarily around

125 to 150 W/m^2 with a few sections dropping below 100 W/m^2. Even those these three houses are within roughly 100 meters of each other and subsequently subject to the same solar conditions, they have drastically different distributions. This notion is most evident when comparing the house on the left to the other two. From these results, shading appears to affect distributions significantly, and as such is one of the most important factors in determining a house's radiation levels.

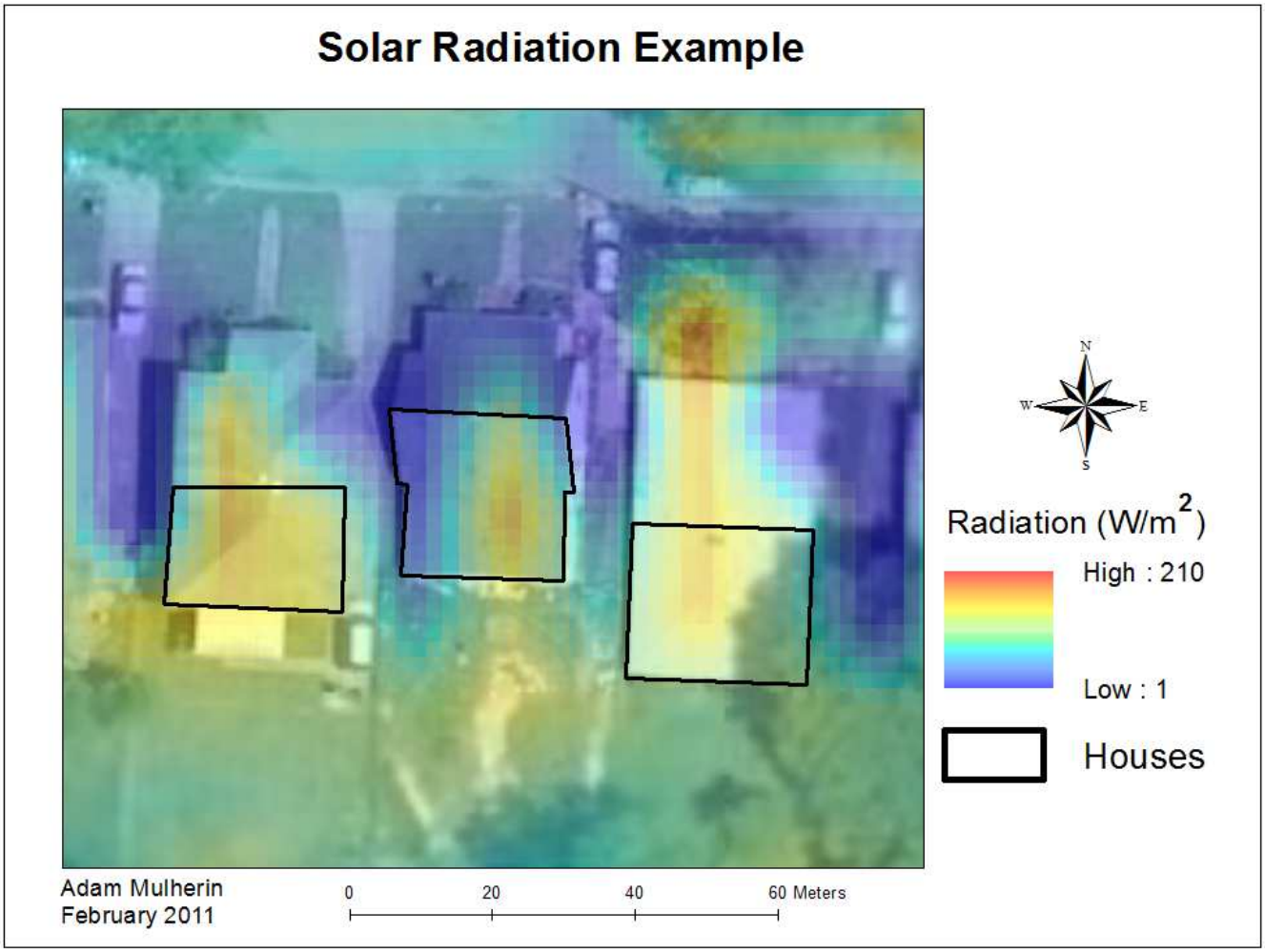

Figure 9 Example of Solar Radiation for Three Homes

2.2 Tool Results

While being able to visually show a homeowner their particular distribution has its merits, the ability to quantify this relationship is also valuable. For this reason, the radiation data discussed above was pooled into a single database for each of the fifty homes as described in section 1.3; the summary of this database is listed in Table 1 (see appendix). Table 1's variables are grouped into three sections: system, financial, and environmental measures. Totals, averages, standard deviations, minimum and maximum values are the statistical measures chosen to analyze the database; each measure is also grouped into the three technology types.

From this table, several observations and trends should be noted. Understandably, technology type significantly impacts the results as each has a different efficiency level and cost, which range from 6.5 and 9% to16% efficiency and $7.50/watt and $9/watt to $10.50/watt for the amorphous, polycrystalline, and monocrystalline respectively. Typically, polycrystalline panels are the most common type used for PV systems; for this reason, the following observations refer to this technology. In terms of power and energy, the average home can expect to have a 2.2 kW system that generates over 4,000 kWh of energy annually. This 2.2 kW system would cost approximately $6,800 after receiving over $12,000 in incentives, which equates to $2.91 per watt. With an average utility savings (annual) of $700 that totals to $17,500 over the expected life of the system (twenty-five years), the backpack period for this average system is a little over nine years. Furthermore, the system would render a 277% return to its owner and produces a net present value worth nearly $16,000. In environmental measures, the system would abate roughly 4,500 pounds of CO^2, 24 pounds of SO^2, and 7 pounds of NO^2 each year of generation.

While giving an overall picture of the study area, these average values can be misleading for systems that deviate around the mean, which is expressed in the standard deviations, minimum and maximum values. For example, certain systems could produce more energy with higher total costs to the homeowner while others are estimated to be smaller and subsequently cheaper. These differences are directly correlated to the amount of solar radiation each system is expected to receive. Consequently, each system has its own unique outputs that merit in-depth examination.

2.2.1 Tool Example

A single house was chosen from the database to discuss the results at a finer scale. The following numbers are referenced in Table 3 (see appendix). Similar to the results discussed earlier, outputs for this home were designated into three categories: system, financial, and environmental analysis. For the system inputs (radiation and roof size), the PV system for this home is predicted to generate over 2,300 kWh for a year. If a homeowner chose to build this 1.3 kW system, it would cost them just over $3,500 at $2.80 per watt, post-incentive. With an average utility savings of $406 per year of generation, the system would break even or pay for itself by its ninth year. According to the financial analysis, the homeowner will receive over the life of the system a ROI of 282% with a NPV $8,762. In terms of environmental impact, the electricity produced off-the-grid from this system is estimated to abate over 2,500 pounds of CO^2, 13 pounds of SO^2, and nearly four pounds of NO^2 for each year of generation.

These are the types of variables a homeowner is considering when investing in a PV system. Based on this analysis, several factors would encourage this homeowner to make the $3,500 investment in the system. Financially this investment is supported by both the ROI and NPV as the person would save money over the life of the system (ROI) while receiving a

positive NPV, which typically serves as the accepted financial indicator. Similarly, if the homeowner has environment concerns, the system would save considerable amounts of CO^2, SO^2, and NO^2 from being released into the atmosphere. This analysis would give most homeowners the reassurance to make this investment.

Compared to the average system in the study area, these values differ considerably. At a total of $3,500 and $2.80/watt, the 1.3 kW system would produce and cost less than the average system, which translates to less benefits and a shorter payback period. Interestingly, the estimated ROI is five percent higher than the mean (282% compared to 277%), however, the NPV indicates a measure of less than half of the average system ($8,762 compared to $15,818). While this investment would pay for itself quicker than most, its return over the life of the system is less as the NPV indicates. This example shows that each system has its own considerations that homeowners should tailor to their specific needs and concerns.

3. DISCUSSION

As expected, the level of solar radiation received at rooftops drastically decreases in areas with significant tree cover. This theory proved correct with the introduction of LIDAR data. At its worst, the effect is detrimental and at best a concern to PV systems. With less solar radiation hitting the panels, the efficiency of an already inefficient technology decreases. More panels would then be needed to supplement similar amounts of energy, which would drive up costs and create longer payback periods. For some projects, this effect could deter a homeowner's investment. In light of these concerns, shading effect need to be taken into account when one constructs a solar project on their roof.

A potential limitation of duplicating this type of analysis is the lack of available LIDAR data. Considering that LIDAR data was the essential input for the 3D surface model, lack of data would be detrimental. Currently, LIDAR is available on a state-by-state basis with only seven having complete data-sets, twelve with partial, and two currently building theirs. While more states are utilizing this technology, over half of the continental U.S. has not even developed partial data-sets, which can be attributed to its costs. Even where LIDAR has been surveyed, professionals might not be aware or have access to data. As mentioned in Directions Magazine: All Things Locations, organizations that are acquiring this extensive data-set are having problems managing it and "providing it to their end users in an effective manner" (Skelton 2010). A solution that has been discussed and partially planned is to create a national LIDAR data-set with consistent standards and availability. The United States Geological Society (USGS) has proposed and researched such a solution. While currently still in the preliminary stages, a national LIDAR data-set would alleviate the limitations discussed here. If it were available, similar analysis as performed here could be performed across wider spaces.

A way to enhance this approach would involve including atmospheric parameters into the modeling phase, such as cloud cover and evaporated water. These two factors can affect radiation levels by changing the area's albedo, i.e. reflective surface. In a general sense, albedo increases as cloud cover and evaporated water content increase. This relationship translates to a higher reflective surface that blocks increasing levels of solar radiation, which means less radiation is penetrating the atmosphere and consequently reaching a PV system. While it would prove difficult to find accurate data to model these parameters, atmospheric variables are important elements to consider when studying the distribution of solar radiation.

The implications of this research for future studies and projects are numerous. Researchers could use a similar methodology to study the relationship between various architectural designs and associated radiation outputs. Theoretically certain types of architecture should translate to higher levels of solar radiation received. Planners and/or developers could then use this information as guidelines to build homes that are better suited for solar PV panels. Another and potentially more significant implication of this study would be its development as an online solar calculator, which can be used to help homeowners with potential PV projects. As mentioned in the introduction, similar web-based tools do exist, such as PV Watts and Solar Calculator. My approach has created outputs that not only tell a homeowner about system outputs, financial concerns, and environmental analysis but where the ideal location is to maximize the output of their PV system. With the groundwork laid, the next step would be developing codes to automate this process for larger areas and subsequently build the web-based interface. The tool's spatial component would set it apart from others while making it intriguing to homeowners.

As argued by Grant Thompson, "there is a great need for accurate solar radiation maps" that can supplement resource managers and public policy with the information needed to plan and predict solar energy in the urban setting (2009). Combining LIDAR data with GIS' modeling capabilities provided an interesting and useful solution to this need. Using this methodology, the analysis showed this approach is able to model shading effects in a 3D environment, which has proven to be an overwhelming variable for solar PV systems. The implications of this research are numerous and significant. As such, this type of analysis should be considered for research that attempts to understand solar energy in space.

4. CONCLUSION

Using the approach of combining LIDAR data and GIS' modeling capabilities presented me with the means to model solar radiation levels in a 3D environment. From analyzing this process, several interesting observations and trends appeared. The first conclusion I drew was the impact that different inputs into the solar analyst had on radiation levels. In the results section, this notion was discussed in detail when comparing "DEM Based" and "LIDAR Based" outputs. The only variable that changed in GIS for these two procedures was the DEM used to create the physical environment to model radiation levels on. As is evident in Figure 6, the "DEM Based" output follows elevation levels closely while the "LIDAR Based" output is far more variable as more features were included in the analysis. Consequently, the interaction between the area's topography and any features above the ground (trees or buildings) in this three-dimensional environment had a significant impact on solar radiation. Along this line of logic, the model's output will be as only good as the raw data used. Errors inherited from the DEM can "lead to errors in the computed values of aspect and slope" which translates to incorrect radiation values (Kumar et al. 1997).

To take this notion further, the interactions exhibited between the terrain's features can drastically affect the yield produced from PV systems. As shown in the maps detailed above, radiation is variably distributed across space. This notion holds for larger areas, such as the study area in question, as well as places as small as a single rooftop. Within area's that are approximately less than 100 m^2, radiation can differ considerably depending on shading effects and a roof's pitch. As such, these interactions must be taken into careful consideration when considering where to place PV panels. From the homeowner's perspective, two well known theories should be heeded: panels should be placed on the southern-facing portions of roofs and

away from trees to avoid shading effects. While these two theories are well accepted and common nature, the results discussed above quantitatively supports them.

Understanding the importance of panel placement is exactly what makes my tool pertinent. When examining the results and methodology in a general sense, one variable is emphasized frequently: how radiation is distributed relative to space. The radiation that hits a roof is particular to that home's situation, i.e. the pitch of the roof and neighboring features. In other words, radiation is relative to each home with certain areas receiving more solar radiation than others. For these reasons, my tool should be approached in relative terms with values that are as close to reality as possible, rather than using the values as exact measurements.

Along this line of thinking, another component that my tool considers is how radiation varies across time. Time was manipulated in the model to include various lengths, such as years, seasons, and a day. By including time as another variable, the approach was able to increase its utility to a homeowner. As shown in Figures 7 and 8 that detail the summer and winter seasons as well as their respective solstices, radiation changes across space and time. While considering yearlong averages as a standard, placement could change if one knows where radiation is greatest for different times of the year, i.e. during summer months. In other words, it provides another piece to consider when deciding where panels should be placed.

In light of these observations, the main conclusion that can be drawn from my analysis is that solar radiation is highly variable across both time and space. Many factors affect how much radiation a house can receive and subsequently the energy output from the PV panels. The tool created here addresses this concern by showing how radiation reacts in the three dimensional environment. For these reasons, my tool could ideally be used as a guide to help a homeowner

decide where the optimum location is for PV panels for their unique situation.

1) **BIBLIOGRAPHY**

"A Consumer Guide to Solar Electricity for the Home." NREL, Jan. 2009. Web. <http://www.nrel.gov/learning/pdfs/43844.pdf>.

Bryan, Harvey, Faia Fases, Hema Rallapalli, and Jin Jo. "Designing a Solar Ready Roof: Establishing the Conditions for a High-Performance Solar Installation." American Solar Energy Society, 2010. <http://www.ases.org/papers/046.pdf>.

Carneiro, Claudio, Francois Golay, Vitor Silva, Corinne Plazanet, and Jong-Jin Park. "GIS and LIDAR Data Analysis for the Integration of Multidimensional Indicators on Urban Morphogenesis Multi-agent Vector Based Geosimulation." *Geocomputation & Urban Planning* (2009).

Carneiro, Claudio, Eugenio Morello, and Gilles Desthieux. "Assessment of Solar Irradiance on the Urban Fabric for the Productoin of Renewable Energy Using LIDAR Data and Image Processing Techniques." *Advances in GIScience* (2009).

"LIDAR Use in a GIS." *NOAA Coastal Services Center*. 2010. <http://www.csc.noaa.gov/products/nchaz/htm/lidtut.htm>.

Kumar, Lalit, Andrew Skidmore, and Edmund Knowles. "Modelling Topographic Variation in Solar Radiation in a GIS Environment." *International Journal of Geographical Information Science* 11.5 (1997): 475-97.

Niket Thakkar, A. Cronin, J. Veatch, D. Cormode, S. PUlver, K. Pounds, W. Henry, "The Effect of Partial Shade on PV Systems", AzRISE 2009.

Pons, Xavier, and Miguel Ninyerola. "Mapping a Topographic Global Solar Radiation Model Implemented in a GIS and Refined with Ground Data." *International Journal of Climatology* 28 (2008): 1821-1834.

Ramachandra T.V., 2007. Solar Energy Potential Assessment Using GIS., *Energy Education Science and Technology*, 18(2): 101-114.

Skelton, Brad. "Managing LIDAR Data." *Directions Magazine - All Things Location*. June 2010. <http://www.directionsmag.com/articles/managing-lidar-data/122358>.

Šúri, Marcel, Huld Thomas, Ewan Dunop, and Heinz Ossenbrink. "Potential of Solar Electricity Generation in the European Union Member States and Candidate Countries." *ScienceDirect*. Oct. 2007.

Thompson, Grant. "Effects of DEM Resolution on GIS-based Solar Radiation Model Output: A Comparison with the National Solar Radiation Database." *OhioLINK ETD*. University of Cincinnati, 6 Nov. 2009. <http://etd.ohiolink.edu/view.cgi/Thompson%20Grant.pdf?ucin1258663688>.

APPENDIX I: Study Area Data

System Measures	*Power (kW)*			*Electricity (kWh/year)*		
Technology	Monocrystalline	Polycrystalline	Amorphous	Monocrystalline	Polycrystalline	Amorphous
Total	146.8	110.1	59.6	267,867	200,900	108,821
Average	2.9	2.2	1.2	5,357	4,018	2,176
Max	7.8	5.8	3.2	14,205	10,654	5,771
Min	0.5	0.4	0.2	882	661	358
St Dev	1.8	1.3	0.7	3,213	2,410	1,305

Financial Measures	*Cost (Total $) after Inc.*			*Cost per Watt*			*Avg. Electrical Savings ($/year)*		
Technology	Monocrystalline	Polycrystalline	Amorphous	Monocrystalline	Polycrystalline	Amorphous	Mono.	Poly.	Amorphous
Total	$ 615,926	$ 341,952	$ 136,171				$ 46,615	$ 34,962	$ 18,938
Average	$ 12,319	$ 6,839	$ 2,723	$ 3.78	$ 2.91	$ 2.27	$ 932	$ 699	$ 379
Max	$ 44,010	$ 24,253	$ 7,204	$ 5.65	$ 4.15	$ 2.62	$ 2,472	$ 1,854	$ 1,004
Min	$ 1,608	$ 1,016	$ 447	$ 1.99	$ 1.66	$ 1.32	$ 153	$ 115	$ 62
St Dev	$ 10,522	$ 5,455	$ 1,673	$ 0.77	$ 0.41	$ 0.14	$ 559	$ 419	$ 227

Financial Measure	*Payback Period (years)*			*Return on Investment*			*Net Present Value*		
Technology	Monocrystalline	Polycrystalline	Amorphous	Monocrystalline	Polycrystalline	Amorphous	Mono.	Poly.	Amorphous
Total									
Average	11.9	9.2	7.1	218%	277%	353%	$ 24,290	$ 15,818	$ 7,587
Max	17.8	13.1	8.3	399%	479%	600%	$ 75,752	$ 48,060	$ 20,099
Min	6.3	5.2	4.2	140%	191%	302%	$ 3,579	$ 2,494	$ 1,248
St Dev	2.4	1.3	0.5	42%	39%	36%	$ 17,636	$ 10,782	$ 4,586

Env. Measure	*CO2 Savings (lbs/year)*			*SO2 Savings (lbs/year)*			*NO2 Savings (lbs/year)*		
Technology	Monocrystalline	Polycrystalline	Amorphous	Monocrystalline	Polycrystalline	Amorphous	Mono.	Poly.	Amorphous
Total	304,029	228,022	123,512	1,577.7	1,183.3	641.0	431.3	323.4	175.2
Average	6,081	4,560	2,470	31.6	23.7	12.8	8.6	6.5	3.5
Max	16,123	12,092	6,550	83.7	62.8	34.0	22.9	17.2	9.3
Min	1,001	751	407	5.2	3.9	2.1	1.4	1.1	0.6
St Dev	3,647	2,735	1,482	18.9	14.2	7.7	5.2	3.9	2.1

Table 1 Database Summary

System Inputs	Solar Input (watts/m2)	Roof Size (m2)	Technology Type
Value	194	54.98	Polycrystalline
System Inputs	Efficiency Standards	Cost ($/watt)	
Value	12%	$9	
Cost/Benefit Inputs	Incentives - Federal	Incentives - State	Incentives - GreenPower Rebate
Value	30%	35% ($10,500 Max)	$.19/kWh
Env. Inputs	CO2 Savings (lbs/kWh)	SO2 Savings	NO2 Savings
Value	1.135	0.00589	0.00161

System Outputs	#1 Est. Power (watts)	#2 Est. Power (kW)	#3 Power (kW)
Value	10,642	10.6	1.28
Equation	Solar Input * Roof Size	Total Power/1000	Efficiency * Total Power

System Outputs	#4 Electricity (kWh/year)
Value	2,331
Equation	System Size * 365 * 5

Financial Outputs	#5 Cost (Total $) before Inc.	#6 Cost (Total $) after Inc.	#7 Cost Per Watt
Value	$11,492	$3,579	$2.80
Equation	Cost/Watt * System Size	Cost - Incentives	Cost/(System Size)
Financial Outputs	#8 First Year Utility Savings	#9 Second Year Savings	
Value	$250	$259	
Equation	0.1076 * Electricity (year)	(1st Year * Inflation Rate (.0378)) * 1st Year	
Financial Outputs	#10 Total Utility Savings	#11 Avg Annual Utility Savings	#12 Payback Period (years)
Value	$10,091	$404	8.9
Equation	Sum 25 Years	Avg of 25 Years	Costs/Electrical Savings
Financial Outputs	#13 Return on Investment	#14 Net Present Value	
Value	282%	$8,772	
Equation	Total Benefits/Total Costs	5% Dicounted Rate	

Env. Outputs	#15 CO2 Savings (lbs/year)	#16 SO2 Savings (lbs/year)	#17 NO2 Savings (lbs/year)
Value	2,645	13.7	3.8
Equation	1.135 * Elecricity	0.00589 * Elecricity	0.00161 * Elecricity

Table 2 Tool Inputs, Equations, and Outputs

System Outputs	Power (W)	Power (kW)	Elecricity (kWh)
Value	1,277	1.3	2,331

Financial Analysis	Costs Pre-Inc ($)	Costs Post-Inc ($)	Cost/Watt ($)	First Yr. Utility Savings ($)	Second Yr. Savings ($)
Value	$11,493	$3,579	$2.80	$251	$259
Financial Analysis	25 Year Savings ($)	Avg. Savings ($)	Payback Period (years)	Return on Investment	Net Present Value
Value	$10,139	$406	8.9	282%	$8,762

Environmental Analysis	CO2 Savings (lbs/year)	SO2 Savings (lbs/year)	NO2 Savings (lbs/year)
Value	2,645	13.7	3.8

Table 3 Tool Example

APPENDIX II: GIS Methods

First Return Clip

1. Clip
    a. Extract LIDAR points for study area

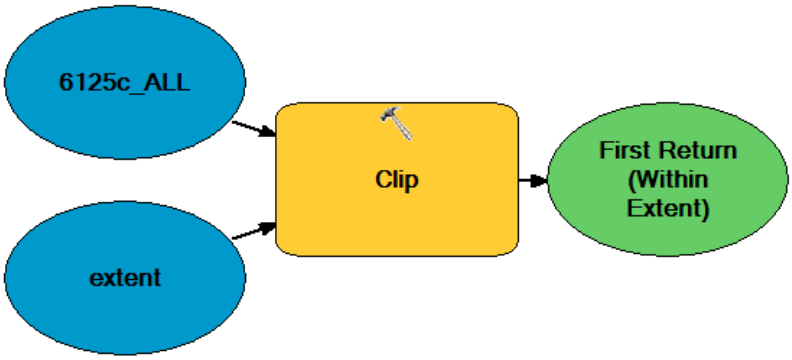

Figure 10 Clipping LIDAR data

Converting First Return to TIN and Raster

1. Create TIN
2. Create Raster

Figure 11 Create 3D Surface

Radiation (Bare-Earth)

1. Clip
    a. Extract DEM for study area
2. Area Solar Radiation
    a. Calculate average daily radiation levels for entire year

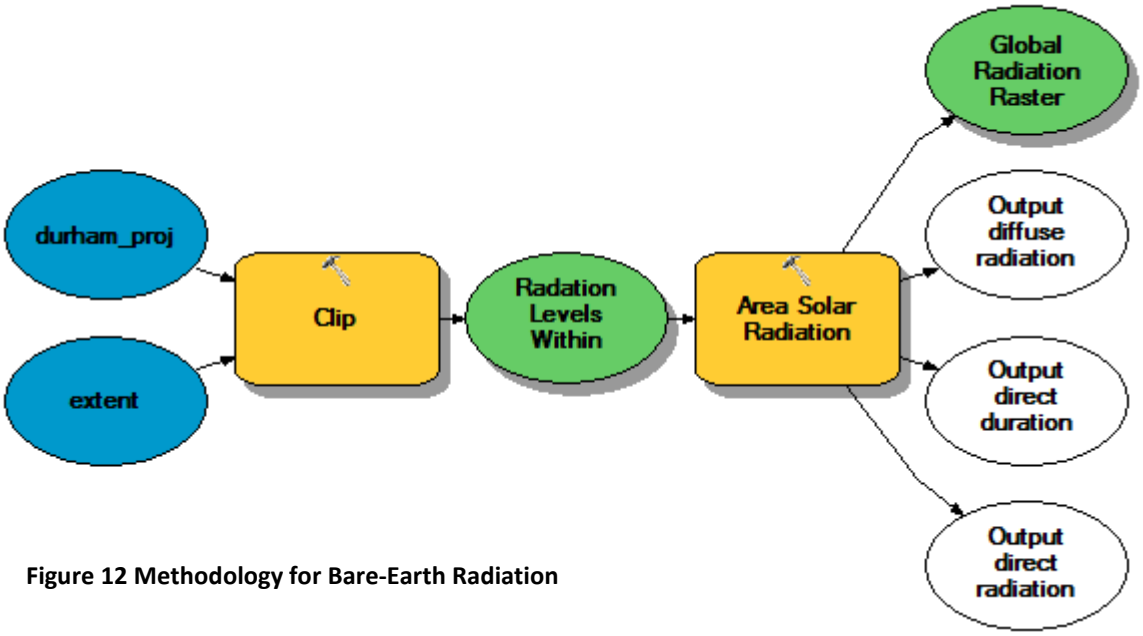

Figure 12 Methodology for Bare-Earth Radiation

Radiation (First-Return)

1. Area Solar Radiation
    a. Calculate average daily radiation levels for entire year
2. Define Project
    a. North American NAD 1983
3. Minus
    a. Subtract bare-earth radiation levels from first-return levels

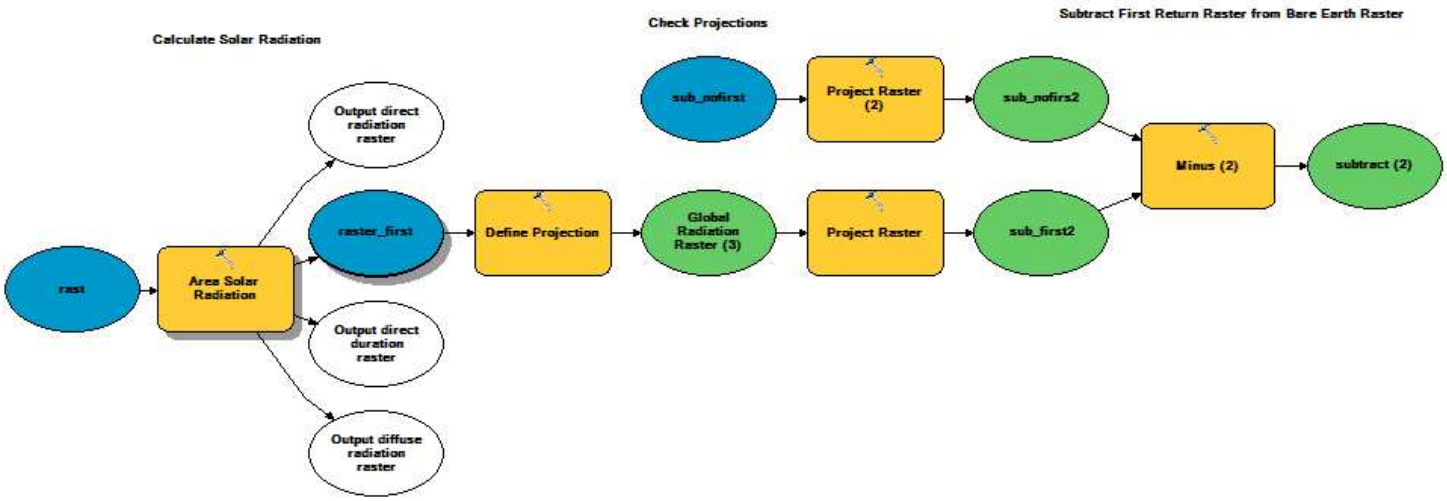

Figure 13 Methodology for First-Return

Zonal Statistics

1. Zonal Statistics as Table
    a. Summarize of radiation raster for each house
    b. Statistic type used : ALL

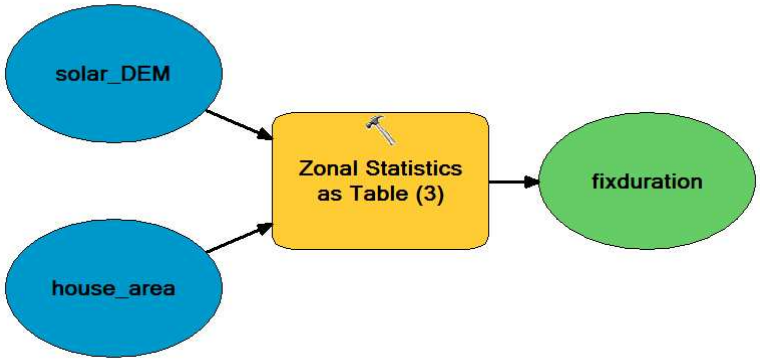

Figure 14 Study Area Statistics